

Analyses of Ligand Binding in Five Endothiapepsin Crystal Complexes and Their Use in the Design and Evaluation of Novel Renin Inhibitors

Elizabeth A. Lunney,*† Harriet W. Hamilton,† John C. Hodges,† James S. Kaltenbronn,† Joseph T. Repine,† Mohammed Badasso,§ Jon B. Cooper,§ Chris Dealwis,§ Bonnie A. Wallace,§ W. Todd Lowther,‡ Ben M. Dunn,‡ and Christine Humble†

Parke-Davis Pharmaceutical Research, Division of Warner-Lambert Company, 2800 Plymouth Road, Ann Arbor, Michigan 48105-2430, Laboratory of Molecular Biology, Department of Crystallography, Birkbeck College, Malet Street, London WC1E 7HX, U.K., and Department of Biochemistry and Molecular Biology, University of Florida, College of Medicine, Box-J245, Health Science Center, Gainesville, Florida 32010-0246

Received March 17, 1993*

Five renin inhibitors were cocrystallized with endothiapepsin, a fungal enzyme homologous to renin. Crystal structures of inhibitor-bound complexes have provided invaluable insight regarding the three-dimensional structure of the aspartic proteinase family of enzymes, as well as the steric and polar interactions that occur between the proteins and the bound ligands. Beyond this, subtleties of binding have been revealed, including multiple subsite binding modes and subsite interdependencies. This information has been applied in the design of novel potent renin inhibitors and in the understanding of structure-activity relationships and enzyme selectivities.

Introduction

The renin-angiotensin system (RAS) has been the target of extensive investigation in cardiovascular research,¹ in particular in the antihypertensive area. Renin, an enzyme produced in the kidney, cleaves angiotensinogen, an α_2 -globulin, to produce angiotensin I. This decapeptide is subsequently cleaved by the angiotensin-converting enzyme (ACE) to yield the potent vasoconstrictor, angiotensin II (AII). Inhibitors of ACE have proven to be successful therapeutic agents in the treatment of hypertension and heart failure,² even though the involvement of ACE in more than one biological system results in uncertainty regarding the complete mechanism of action for the inhibitors. A second means of intercepting the RAS process is through binding antagonists at the AII type 1 receptor.³ Non-peptide analogs that act through this mechanism are currently in clinical trials. One concern in this approach is the increased concentration of unbound angiotensin II in the system and possibly its effect on the AII type 2 receptor, although the function of this latter receptor is still unclear.⁴ A third strategy to disrupt the cascade is to inhibit the renin enzyme and block the production of angiotensin I, which is the rate-determining step in the RAS process. Human renin binds selectively to human angiotensinogen and is thus an attractive target to inhibit. Initially, due to lack of purified material, no crystal structure of human renin was available to aid in this research. As an alternative, crystallographic studies of the homologous fungal enzyme, endothiapepsin, were undertaken.^{5,6}

Endothiapepsin, derived from *Endothia parasitica*, and renin are members of the aspartic proteinase class of enzymes,⁷ which also includes cathepsin D and E, pepsin, gastricsin, chymosin and the fungal enzymes from *Penicillium janthinellum* and *Rhizopus chinensis*. The aspartic proteinases are comprised of two structurally

similar lobes; each lobe contributes an aspartic acid residue to form the catalytic diad where the substrate peptide bond is cleaved. The binding site is a groove or cleft formed by the N- and C-domains, which are mainly comprised of β -strand structures. The cleft is covered by a flexible β -hairpin "flap" segment in the N-domain,⁸ and evidence exists for a rigid body movement of the C-terminal domain⁹ upon ligand binding.

In this study, endothiapepsin was cocrystallized with analogs designed as renin inhibitors.^{5,10} The analyses of endothiapepsin crystal structures have provided critical data for the rule-based construction of a human renin model^{11,12} that was continually refined to incorporate newly determined experimental information. Beyond this, valuable insight regarding the ligand occupation of the renin binding site and the hydrogen-bonding interactions occurring between the enzyme and various inhibitors was gained. The experimental data guided, validated, and helped develop modeling methodologies¹³ to dock ligands in our renin models and to design novel inhibitors. Simultaneously, rationales for structure-activity relationships and selectivities could be developed. Herein we report the analyses of ligand binding in five endothiapepsin crystal structures complexed with analogs designed as renin inhibitors. The application of the extensive information provided by the crystal structures toward the design and evaluation of novel renin inhibitors will be discussed.

Results

Inhibitors. All five renin inhibitors cocrystallized with endothiapepsin are peptide/peptidomimetics (Table I), which span the binding site of the enzyme with P₄ to P₁' substituents¹⁴ (Figure 1). Analogs 2, 3, and 4 extend further to the P₂' site, while 1 continues to the P₃' position. Across the series of ligands, the P₄ to P₁ residues bind in an extended conformation (Table II). The amide bonds form conserved hydrogen bonds with the enzyme, while the P₄ to P₁' side chains occupy subsites alternating on either side of the backbone. At the P₁-P₁' site, which is the cleavage target in the substrate, the inhibitor structures present various transition-state mimetics of the hydrolysis process, while binding a hydrophobic group in the S₁

* Parke-Davis Pharmaceutical Research, Division of Warner-Lambert Company.

† Laboratory of Molecular Biology, Department of Crystallography, Birkbeck College.

‡ Department of Biochemistry and Molecular Biology, University of Florida, College of Medicine.

§ Abstract published in *Advance ACS Abstracts*, October 15, 1993.

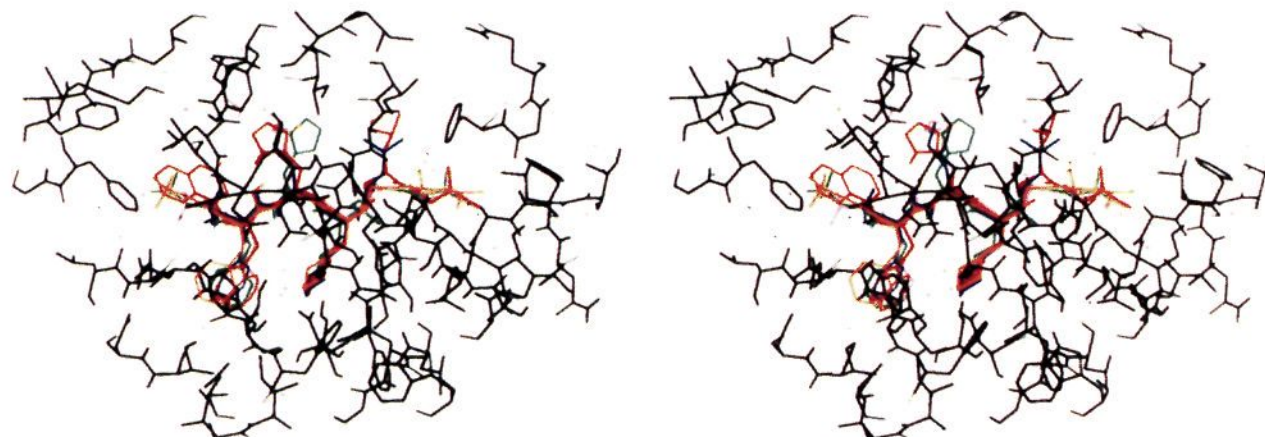


Figure 1. Overlap of the inhibitors bound in the endothiapepsin cleft (residues within 8 Å of inhibitor 1, black): 1, orange; 2, red; 3, green; 4, purple; 5, blue. The key water molecules are labeled in red: WAT1, WAT2, ...

Table I

	ligand binding							binding affinities	
	P ₄	P ₃	P ₂	P ₁	P ₁ '	P ₂ '	P ₃ '	endothiapepsin K _i (nM)	renin
									human plasma IC ₅₀ (nM)
1.								16000	22
2.								240	170
3.								110	3.3% (10 ⁻⁶ M)
4.								69	25
5.								6.5	0.1 ^a

^a Renin monkey plasma.

Table II. Backbone Torsion Angles

compd	P ₃		P ₂		P ₁	
	φ	ψ	φ	ψ	φ ^a	ψ ^a
1	-107.0	126.6 ^a	-126.4 ^a	109.6	-125.9	64.9
2	-67.3 ^a	151.7	-132.6	99.8	-107.5	45.5
3	-70.0	150.6	-140.2	74.7	-115.4	74.2
4	-83.6	144.7	-136.3	88.2	-130.8	64.2
5	-102.9	142.4	-149.4	91.0	-109.1	59.4

^a Angles analogous to φ or ψ angles.

pocket. Inhibitors, 1, 3, and 4 contain statine or statine derivatives at this position. (Statine is a moiety that has five atoms in its backbone structure and has been shown to replace two amino acids.¹⁵) These residues have either an isobutyl or a cyclohexylmethylene P₁ substituent and contain no P₁' side chain. A phosphinate group is incorporated as the transition-state mimetic in the phosphostatine residue in 3. The remaining analogs, 5 and 2,

contain a diol or a hydroxyethylene isostere¹⁶ as the transition-state mimetic, a cyclohexylmethylene P₁ substituent, and a P₁' side chain. Focusing on the P₄ position, 4 and 5 contain sulfonyl derivatives (the morpholine in 5 is not defined by the X-ray data), 2 presents a naphthylene and the remaining analogs have BOC¹⁷ groups. The P₃ position in all the inhibitors introduces an aromatic group in the S₃ binding site generally through a Phe residue. One of the ligands, 1, contains an hydroxyethylene isostere in place of an amide linkage at the P₃-P₂ junction.^{18,19} At the P₂ site, His is present in 2 and 3, while the other ligands have the following residues: a flexible Lys^{20,21} derivative (4), an α-thio amino acid²² (5), and a Gly with no side chain (1). For the inhibitors which extend to the P₂' site, a branched alkyl group is projected into the S₂' pocket either through a Leu or an MBA¹⁷ residue. An AMPMA¹⁷ group is found in the P₃' position of 1, which is the only inhibitor extending to this site. The P₃' moiety is not defined by the X-ray data beyond the amide nitrogen.

Grin/Grid²³ calculations, a method of identifying potential polar and hydrophobic interaction sites on a target molecule using probe groups, were carried out with the inhibitor crystal structures.

Hydrogen Bonding. The extended conformations of the bound ligands (Figure 1) are stabilized on one side by residues found in the enzyme "wall" (Gly-34, Gly-217, and Thr-219) and on the other by residues in the flexible hairpin "flap" (Gly-76 and Asp-77) (Figure 2). The transition state mimetic binds to the catalytic diad (Asp32 and Asp215). The Grin/Grid calculations determined for inhibitor 4 using a water probe clearly identify the potential, polar interaction sites (Figure 3) and is representative of the results obtained for the other inhibitors. These polar sites run parallel to the backbone on either side of the ligand, and as will be shown, most of these interaction sites are satisfied by either the flap or wall region of the enzyme described above. The overall hydrogen bonding network for the structures is shown in Figure 4 with the distances listed in Table III.

The inhibitor structures contain up to seven conserved hydrogen bonds from the P₃ to P₂' sites, excluding the diad hydrogen bonding complex. Hydrogen bonds are consistently formed between Thr-219(OH) and the P₃-(NH), except for 2 which lacks an amide NH at the P₃ site. The distances range from 2.6 to 3.0 Å. A second hydrogen bond is conserved between Thr-219(NH) and the P₃(CO) or in the case of 1, the P₃(OH) of the hydroxyethylene isostere. At the P₂ site, a bifurcated interaction is conserved between the flap Asp-77(NH) and Gly-76(NH) and the P₂(CO), while at P₁, a hydrogen bond between Gly-217(CO) and the P₁(NH) is consistent across the series.

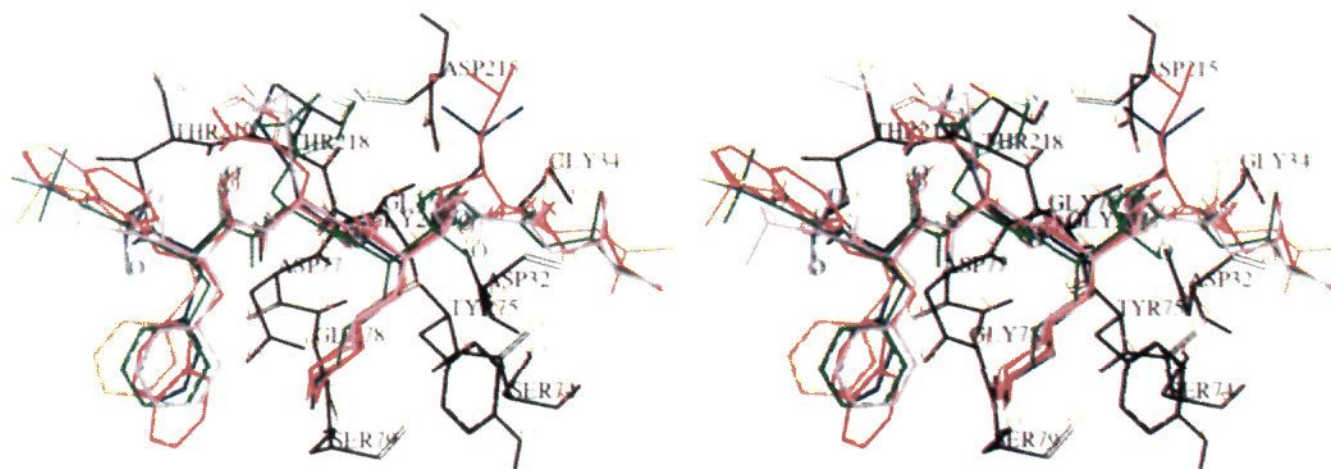


Figure 2. The inhibitor crystal structures (1, orange; 2, red; 3, green; 4, purple; 5, blue) with cleft residues from complex 1 (black). Polar hydrogens were added using Sybyl.³⁹

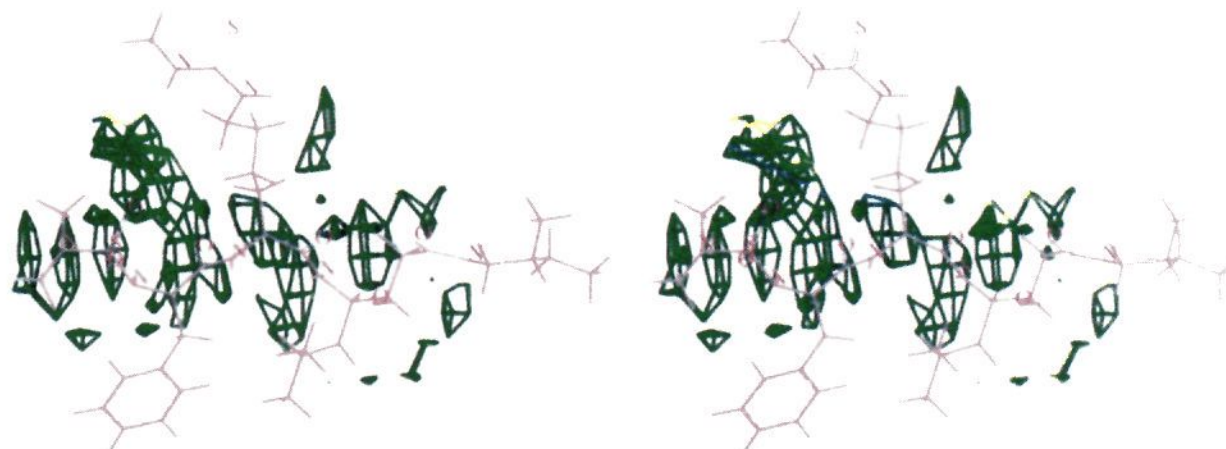
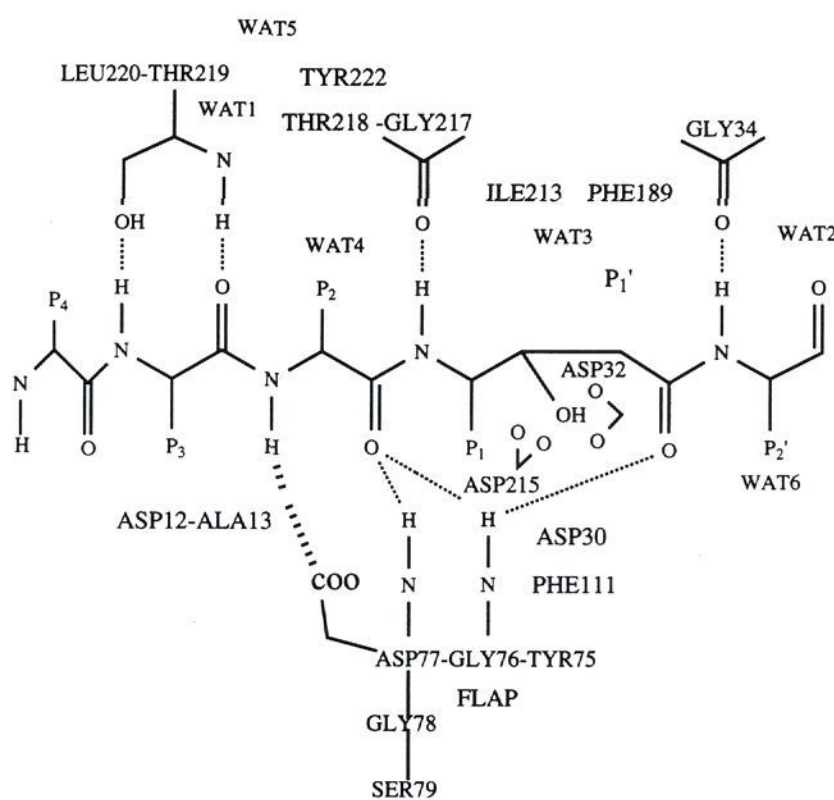


Figure 3. Potential polar interaction sites: contour of Grin/Grid calculations for 4 using a water probe at -4 kcal/mol energy level. Hydrogens were added using Sybyl.³⁹



(..... Non-conserved hydrogen bond)
(———— Conserved hydrogen bonds)

Figure 4. The hydrogen-bonding scheme between inhibitor and endothiapepsin binding site. The general positions of the water molecules (WAT1, WAT2, ...) are shown.

These three hydrogen bonds have distances that range either from 3.1 to 3.3 Å or 3.1 to 3.4 Å. One interaction involving the peptide backbone that is not conserved across the series occurs at the P₂ site. Only 4 and 5 form a hydrogen bond between Asp-77(COO) in the flap and the P₂(NH). The comparative analysis of the crystal structures (Figure 5) reveals a shift of the Asp-77 side chain to within hydrogen-bonding distance of the ligands 4 and 5. This interaction, however, notably alters the intramolecular distance between Asp-77(COO) and either Ser-79(NH) or

Table III. Hydrogen Bond Distances^{a-c}

inhibitors	1	2	3	4	5
Thr-219(OH)-P ₄ BOC(O)	3.5	NA	3.4	NA	NA
Thr-219(OH)-P ₃ (NH)	2.6	NA	2.7	2.8	3.0
Thr-219(NH)-P ₃ (CO)	3.1 ^d	3.0	3.1	3.0	3.0
flap Asp-77(COO)-P ₂ (NH)	NA	NO	NO	3.0	3.5
flap Asp-77(NH)-P ₂ (CO)	3.2	3.4	3.3	3.1	3.2
flap Gly-76(NH)-P ₂ (CO)	3.3	3.2	3.4	3.1	3.1
Gly-217(C=O)-P ₁ (NH)	3.2	3.3	3.2	3.3	3.1
flap Gly-76(NH)-P ₁ '(CO)	2.7	3.1	2.7	2.9	2.9 ^d
Gly-34(CO)-P ₂ '(NH)	3.0	2.7	3.2	2.8	NA
Ser-74(CO)-P ₃ '(NH)	3.1	NA	NA	NA	NA
total	9	6	8	8	7

^a NA = not applicable. ^b Does not include Asp-215 and Asp-32 hydrogen bonds. ^c X-H...Y angles are all $>90^\circ$ and the X-Y distance ≤ 3.6 Å. ^d Hydroxyl group is a hydrogen acceptor.

Ser-79(OH) observed in 1. (Since 1 does not have a polar group at P₂ influencing the orientation of the Asp-77 side chain, it is considered a reasonable reference to measure the effect of the ligand hydrogen-bond interaction.) For 4, which forms a strong hydrogen bond with Asp-77(COO) (Table III), the distance between Asp-77(COO) and Ser-79(NH) expands from 2.9 to 3.3 Å. Completing the conserved hydrogen bonding scheme are the two interactions on the C-terminal portion of the inhibitors. These involve Gly-76(NH) in the flap and the P₁'(CO), or in the case of 5, the P₁'(OH), and secondly, Gly-34(CO) and the P₂'(NH). (Analog 5 with no P₂' group cannot form the latter interaction.) The interaction distances are 2.7–3.1 and 2.7–3.2 Å, respectively.

All the analogs place an oxygen of the transition-state mimetic between the Asp-215(COO) and Asp-32(COO) at the active site (Figure 6). These enzyme side-chain carboxyl groups are aligned essentially in a plane, as indicated by their RMS deviations (Table IV). The distances between the ligands and the diad carboxyl groups are listed in Table IV and have been designated

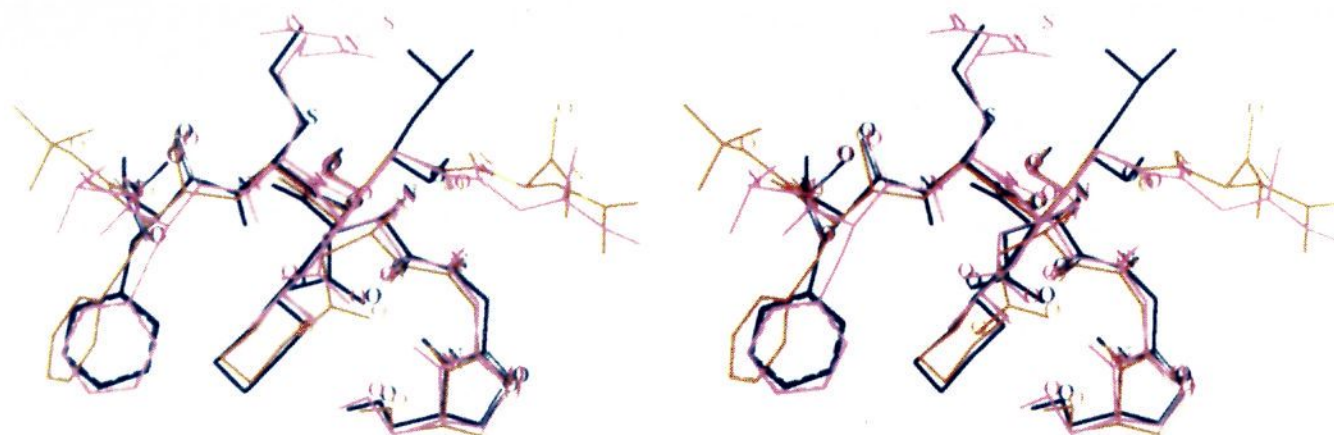


Figure 5. Overlap of inhibitors and the "flap" residues Asp-77-Ser-79 (1, orange; 4, purple; 5, blue).

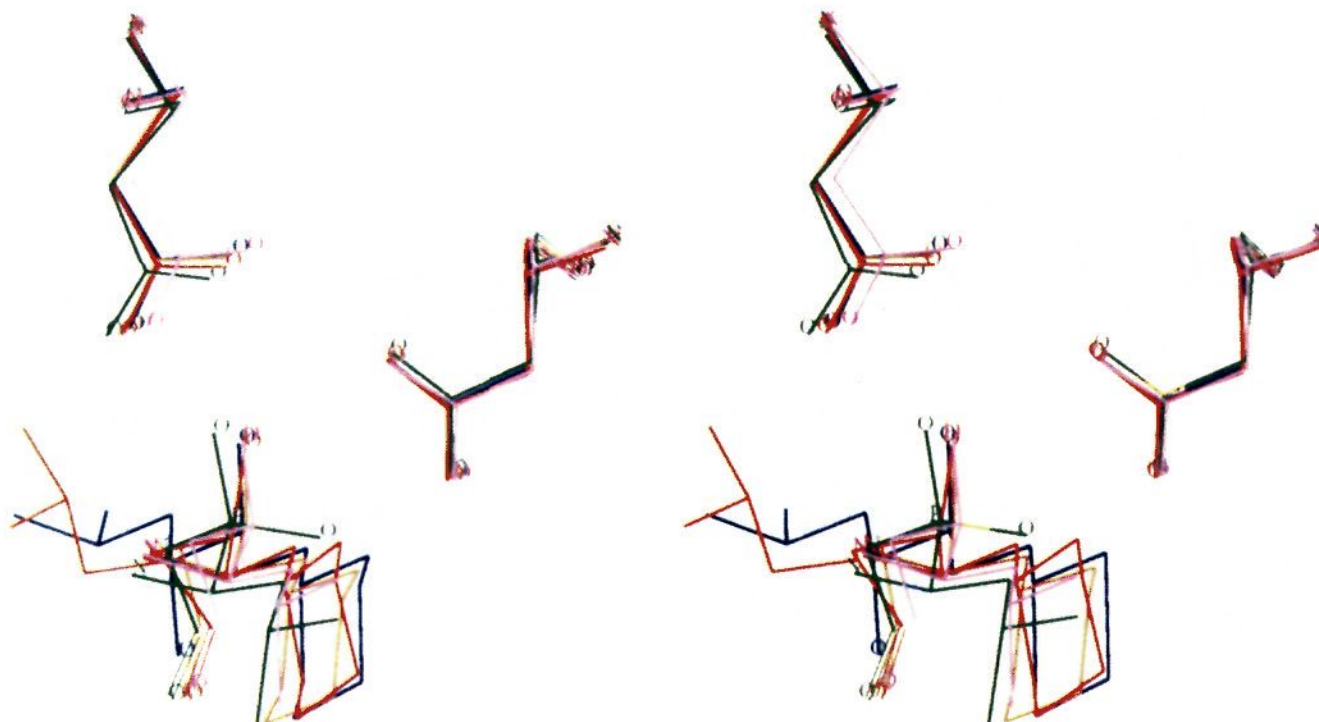
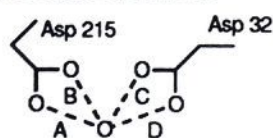


Figure 6. View of the P₁ oxygens of the inhibitor P₁-P₁' groups oriented between the two carboxyls of the catalytic diad (1, orange; 2, red; 3, green; 4, purple; 5, blue).

Table IV. Hydrogen Bond Distances



inhibitor	distances				RMS deviation (Å) ^b
	A	B	C	D	
1	2.6	2.8	2.6	3.3	0.118
2	2.7	2.9	2.7	3.2	0.101
3	2.8	2.5	3.1	3.8 ^a	0.081
4	2.6	3.0	2.6	3.4	0.103
5	2.6	3.0	2.7	3.4	0.116

^a Beyond hydrogen bond distance. ^b Fit of Asp-215 (COO) and Asp-32 (COO) to a plane defined by the six atoms of the COO groups.

A, B, C, and D. The lengths of these interactions form a conserved pattern across the series of inhibitors with the exception of **3**, the phosphostatine derivative. Excluding **3** from the analysis, the closest contacts are consistently A and C, involving the Asp-215 outer oxygen and the Asp-32 inner oxygen, respectively. In three cases, identical distances are found for A and C. In **3**, the oxygen between the carboxylic groups is oriented further away from Asp-32 than the P₁ hydroxyl oxygen in the other inhibitors. With this inhibitor the smallest interaction distance is B, involving the Asp-215 inner oxygen and the longest distance observed is D, which falls outside of the hydrogen-bonding range. However, this oxygen in **3** can still interact with the inner Asp-32 oxygen. In addition, the second oxygen bound to phosphorus is within hydrogen bonding distance of both Asp-32 oxygens.¹⁰

Unique interactions are observed at the P₄ and P₃' sites. The only polar interactions with the enzyme found for the P₄ groups are the hydrogen bonds formed between Thr-219(OH) and the urethane oxygen of the BOC groups in **1** and **3**. However, the interaction distances indicate weak hydrogen bonds. A polar interaction is also observed for Ser-74(CO) and the P₃'(NH) in **1**, the only inhibitor that extends to this site.

The only ligand side chains in the crystal structures that have the capability of hydrogen bonding are at the P₂ site. None of these side chains participate in direct polar interactions with the enzyme, although in a protonated state, the π nitrogen of the His in **2** can interact intramolecularly with the P₃(CO).

The total number of hydrogen-bond interactions between the inhibitor and the enzyme observed in the crystal structures (excluding the interactions with the diad) vary from six interactions for **2** to nine for **1**. From the P₃ to P₂' sites, seven conserved hydrogen bonds are identified, dependent on the preservation of the required functionalities. Overall, in this set of interactions the shortest distances are observed for the Thr-219(OH) to P₃(NH) hydrogen bond, followed by those involving the "prime" side residues in the ligand. Conversely, the longest distances are found for the bifurcated hydrogen bond to the flap and the Gly-217(CO) to P₁(NH) interaction. With regard to the ligands, all the intermolecular hydrogen bonds involve backbone groups. These interaction sites were identified by the Grin/Grid calculations. No inhibitor side chain participates in direct polar interactions with

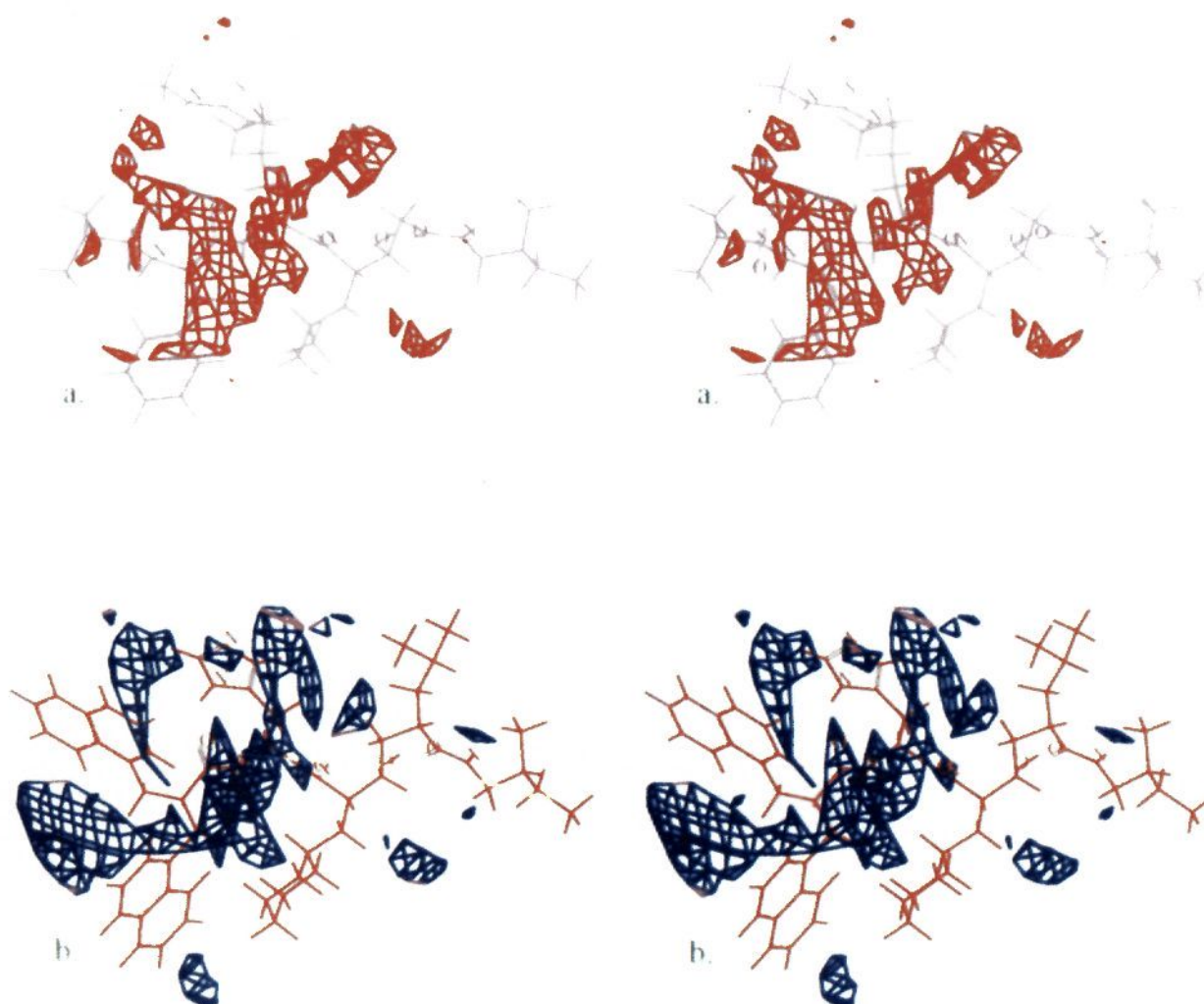


Figure 7. Potential hydrophobic interaction sites: contour of Grin/Grid calculations for 4 (a) and 2 (b) using a methyl probe at -1.5 kcal/mol energy level. Hydrogens were added using Sybyl.³⁹

the enzyme, whereas the enzyme side chains of Thr-219 and Asp-77, as well as the catalytic aspartic acids Asp-215 and Asp-32, do hydrogen bond with the ligands.

Bound Water Molecules. The potential interactions of the resolved water molecules (designated WAT1, WAT2, ...) with the ligands and enzyme were assessed in the crystal structures. Every crystal structure shows WAT1 above the P_3 site (Figures 1 and 4). This molecule is within hydrogen bonding distance of Tyr-222(OH), Leu-220(NH), and Thr-219(NH) in all the crystal structures. With regard to the ligands, WAT1 can interact with the P_4 groups in 1, 4, and 5, the His imidazole in 2, as well as the P_3 (CO) or P_3 (OH) groups in all the inhibitors. WAT5 can contact Tyr-222(OH) in all the crystal structures and also the P_2 thiourea group of 4, while WAT2 is within hydrogen bonding distance of the P_2' (CO) in 1.

WAT3, WAT4, and WAT6 fill in subsites not occupied by the inhibitor. With the statine-type derivatives, 1, 3, and 4, WAT3 resides in the S_1' site and can interact with the P_2 imidazole in 3. WAT4 is found in the S_2 site in 1, while in 5 WAT6 resides in the S_2' pocket and can hydrogen bond to the P_1' (OH).

In summary, WAT1 can interact with the enzyme and inhibitor in all the crystal structures. Four of the inhibitors, 1, 3, 4, and 5, can also form a hydrogen bond with one of the other water molecules. WAT3, WAT4, and WAT6 reside in pockets not occupied by the inhibitor.

Subsite Occupation. The subsite occupation by the ligands was analyzed using an alignment of the enzyme crystal structures determined by least-squares fitting²⁴ (Figure 2). The Grin/Grid calculations with a methyl probe carried out for 4, which are representative of the analyses of the other inhibitor crystal structures, nicely highlight the location of the hydrophobic interaction sites predominantly toward the amino terminus of the inhibitors (Figure 7a). This result is partly influenced by the orientation of

the P_1 groups uniformly toward the N-terminus and, in 2 and 4, the positioning of the P_2 side chains in the same general direction.

The P_4 , P_2 , and P_1' substituents of the inhibitors occupy an area on the same side of the backbones of the bound ligands (Figure 2). The S_4 subsite borders on residues Thr-219 and Leu-220. The P_4 sulfonyl groups of 4 and 5 overlap, and in each inhibitor, one of the sulfonyl oxygens hydrogen bonds to WAT1, while the other does not form polar contacts with either the enzyme or a water molecule. In comparing the P_4 BOC groups in 1 and 3, the *tert*-butyl segments are found to be in a staggered orientation relative to one another. The hydrophobic contribution of the P_4 naphthyl group in 2 is evident in Figure 7 (parts a and b), which shows the comparison of this moiety with the BOC group of 4 using the Grin/Grid analysis and a methyl probe.

The S_2 pocket is comprised of Gly-76, Asp-77, Thr-218, and Tyr-222. At this site, different orientations of the His side chains are seen in 2 and 3²⁵ (Figure 2). With 2, the imidazole ring is oriented toward the P_4 site, as opposed to P_1' as observed in 3. In 4 and 5, the P_2 groups are positioned directly above the P_2 α -carbon, with the Lys derivative of 4 extending out over the flap biased toward the P_4 site.

Phe-189, Ile-213, and Gly-76 surround the S_1' binding region. Only two inhibitors occupy this enzyme pocket; the P_1' alkyl side chain in 2 aligns with the terminal alkyl group in 5.

The P_3 and P_1 binding sites are located on the same side of the backbone, directed approximately 180° from the P_4 , P_2 , and P_1' sites. Asp-12, Ala-13, and Thr-219 surround the S_3 pocket, while the S_1 site borders on Asp-30, Gly-217, Phe-111, and the diad, Asp-215 and Asp-32. In the S_3 site, various orientations of the aromatic groups are seen across the series.⁵ On closer inspection, these can be grouped into three families (Figure 2). Inhibitors 4 and

3 position their phenyl groups pointing edge-on to the P₁ side chain, while 2 and 5 orient the P₃ aromatic groups toward the enzyme flap. In 1, the phenyl group is situated more toward the opening of the binding region than are the other aromatic side chains.

In analyzing the P₁ alkyl side chains of the inhibitors, the isobutyl groups of 3 and 4 are oriented slightly closer to the flap region than the cyclohexylmethylene groups in the other inhibitors.

In completing the analysis, the P₂' side chains extend in line with the backbones in a pocket bordered by Gly-34 and Tyr-75. At this site, the MBA¹⁷ alkyl groups in 2, 3, and 4 align and in turn overlap with the Leu side chain in 1.

Discussion

Ligand Binding. The X-ray crystal complexes reveal a conserved hydrogen bonding scheme between the backbone chain of the inhibitors and the protein (Figures 2 and 4). Focusing first on the interactions not involving the catalytic aspartic acids, particular trends are observed in the hydrogen-donor/acceptor roles of residues in different regions of the enzyme and the interaction distances for the individual hydrogen bonds conserved across the series (Table III). Interestingly, the conserved hydrogen bonds with the flap locate the hydrogen acceptor groups in the ligand and the donor participants in the enzyme. With the exception of the Thr-219(NH) to P₃(CO) interaction, the opposite appears for the hydrogen bonds formed with the wall residues, with the ligand supplying the donor component and the enzyme wall providing the acceptors.

As described above, the longest conserved hydrogen bonds occur between the flexible flap and the P₂ residue on one hand, and between Gly217 and the P₁(NH) on the other. This would be expected for the former, which involves a bifurcated hydrogen bond. It is intriguing that both interactions involve the amide bond located at a central point in the bound ligand, adjacent to the catalytic site.

Conversely, the hydrogen bond presenting overall the closest interaction distances occurs between Thr-219(OH) and the P₃(NH). Surveying this interaction across the inhibitor series, the longest distance is observed for 5, at 3.0 Å. Since 4 forms a hydrogen bond of 2.8 Å, the sulfonamide group does not appear to be the reason for the larger distance observed with 5. Alternatively, the bulky morpholine group in 5, which is not defined by the X-ray data, may force the inhibitor away from the enzyme wall, resulting in the longer distance.

The hydrogen bond between the flap Gly-76(NH) and the P₁'(CO) also ranks among the shortest observed. Four inhibitors interact with a distance less than or equal to 2.9 Å, while 2 forms a hydrogen bond with a distance of 3.1 Å. Analog 2 has a hydroxyethylene isostere at the P₁-P₁' site, while the other inhibitors contain statine derivatives or the diol isostere, in which the P₁' hydroxyl of the isostere participates in the flap interaction. The carbonyl group interacts more closely with Gly-76(NH) in the statine-type derivatives than in the second residue of the isosteric dipeptide replacement, where it is oriented further away. Conversely, this latter group allows the P₂'(NH) to form a shorter hydrogen bond with Gly-34(CO) than is observed with the other inhibitors. Therefore, the binding energy that may be lost in the interaction of Gly-76(NH) with 2, relative to other inhibitor complexes, may be at least

partially recovered through the Gly-34(CO) hydrogen bond. This variation in binding for the different types of transition-state mimetics may be indicative of their ability to inhibit, although further studies are necessary to fully investigate this premise.

Besides the interaction of its side chain hydroxyl group, Thr-219 is also involved in a conserved hydrogen bond between its amide NH and the P₃(CO). This latter contact has the most consistent interaction distance across the series of inhibitors, including 1 with the hydroxyethylene isostere. The crystal complex with 1 definitively shows the ability of the isostere hydroxyl group to mimic the carbonyl of an amide bond and act as a hydrogen acceptor with Thr-219(NH).

The largest distance variance is observed in the conserved hydrogen bond between Gly-34(CO) and P₂'(NH) (2.7–3.2 Å) and can be linked to the P₁-P₁' substituent. The phosphostatine derivative 3 with the MBA group at P₂' has the largest bonding distance. The other MBA containing analogs, 2 and 4, bind 0.5 and 0.4 Å closer, suggesting that the phosphinate moiety is effecting the larger interaction distance for this hydrogen bond. However, simultaneously, the distance between the Gly-76(NH) in the flap and the P₁'(CO) in 3 is one of the shortest measured for this hydrogen bond and may be somewhat counterbalancing the effect of the Gly-34(CO) interaction.

For the P₁-P₁' diol derivative 5, the interaction of the P₁' hydroxyl with the flap is quite revealing. It had been proposed that this hydroxyl interacted with Asp-215²⁶ in renin; however, subsequent structure-activity relationship analysis of renin inhibitors with oxygen-containing ring systems at P₁' indicated that the hydroxyl group acted as a hydrogen acceptor.²⁷ The endothiapepsin crystal complex with 5 clearly shows a hydrogen acceptor interaction with the flap and perhaps suggests the existence of an analogous interaction in renin. This flap interaction also directs the alkyl portion of ACDMH¹⁷ to bind in the S₁' subsite, resulting in the overlap observed with the P₁' group in 2.

The close multiple interactions between the transition-state mimetics and the catalytic aspartates (Table IV) represent the tightest binding between the inhibitors and the enzyme. This observation along with the discovery that the longest hydrogen bonds in the complexes exist between the adjacent amide bond at P₂-P₁ may be clues to the binding mechanism that occurs between the ligands and the enzyme. It suggests that the binding of the transition-state mimetic at the active-site diad is the primary site of association, and thus the most favorable binding mode for this catalytic site complex takes precedence over the other interactions. This emphasizes the importance of the complementarity of the ligand-enzyme complex at the active site in the design of novel potent renin inhibitors.

Table IV shows the RMS deviation from planarity for the catalytic carboxyls in all the inhibitor complexes. Interestingly, 3, the phosphostatine derivative, has the configuration closest to planarity and as can be seen from Figure 6 also shows a shift in the orientation of the Asp-215 side chain toward Thr-218 relative to the other inhibitor complexes. This configuration results from the accommodation of the two oxygens of the phosphinate group at the P₁-P₁' site.

The crystal complexes also offer detailed information regarding the subsite occupation by the inhibitor side chains. Multiple binding modes possible within each subsite as well as the dependencies transmitted between groups residing at different subsites are revealed. Analogs 2 and 3 bind with different orientations of the His side chain in the S₂ pocket. The P₂ group in 2 is oriented toward the S₄ site, while in 3 the side chain is directed toward the S₁' pocket. Upon further inspection, it is noted that 2 has an isobutyl P₁' substituent, while 3 has no side chain at this position (Figure 2). Thus the presence of this P₁' group appears to orient the imidazole away from the S₁' site, which is indicative of the interdependencies that can exist between subsites.

A second illustration of this phenomenon exists for the P₃ and P₁ substituents. As described above, the P₃ side chains can be categorized into three separate conformational families. Analog 3 and 4 show an edge-on positioning of the phenyl groups with the P₁ side chains, while the P₃ aromatic groups in 2 and 5 are directed more toward the flap region (Figure 2). This shift in orientation results from the bulky P₁ cyclohexyl group in 2 and 5, which induces a twist of the P₃ side chain.⁵ A cyclohexyl group is also found at P₁ in 1; however, its phenyl group is projected further away from the S₁ site. The reason for such a shift may lie in the isosteric replacement at the P₃-P₂ linkage, which alters the backbone geometry and increases the flexibility of the ligands.

At the P₁ site, the isobutyl groups of 3 and 4 are oriented slightly closer to the flap than the cyclohexylmethylene groups in the other inhibitors. This side-chain orientation would apparently be prohibited with the bulkier cyclohexyl group due to a contact with Asp-77. Nonetheless, the S₁ pocket can accommodate the larger cyclohexyl group, which offers increased hydrophobic binding and van der Waals (vdW) interactions with the enzyme relative to the isobutyl moiety.

Binding Activity: Endothiapepsin. The binding affinities for the inhibitors with endothiapepsin and renin are listed in Table I. The endothiapepsin activities vary from nanomolar to greater than micromolar. Although the analogs in the series comprise a diverse group of ligands, certain elements can be identified as impacting the binding affinities. Beyond the common interactions with the diad, the most potent endothiapepsin inhibitors, 5 and 4, form seven and eight hydrogen bonds with the enzyme, respectively (Table III). Analog 4 contains all seven conserved hydrogen bonds, while 5, in not extending to the P₂' site, does not interact with Gly-34. These are the only ligands that show favorable contacts between the P₂(NH) and Asp-77(COO) in the flap region, although as indicated above, intramolecular interactions between Asp-77 and Ser-79 in the protein are affected and may weaken the binding energy. Analogs 5 and 4 also have in common a sulfonyl group at P₄, which binds to the enzyme through WAT1. The stronger potency of 5 relative to 4 may be linked in part to the cyclohexylmethylene group at P₁, which can occupy the site more fully than the smaller isobutyl group in 4²⁸ and thus provide increased vdW interactions and hydrophobic binding. In addition, the less flexible P₂ residue in 5 does not have the unfavorable entropic factor affecting binding that is inherent in the Lys derivative in 4. The next two inhibitors in the order of potency, 3 and 2, have His at the P₂ position and bind in the 10⁻⁷ M range. The less potent activity observed

with 3 could be linked to the phosphostatine moiety. The phosphinate may be less well accommodated at the active site than a hydroxyl group bound to an sp³ carbon and thus a less favorable transition-state mimic. The shift of Asp-215 relative to the other inhibitor complexes described above may be indicative of this, and the energy cost in disrupting this region may be reflected in weaker binding. Furthermore, the lower activity of the phosphostatine derivative can be linked to the smaller isobutyl side chain at P₁. Relative to 4, the 4-fold drop in potency with 2 may be partly traced to the inhibitor having only six direct polar interactions with the enzyme. The Thr-219(OH) to P₃(NH) interaction is lost due to the bis-naphthyl group at P₃-P₄. The weakest inhibitor, 1, surprisingly has nine polar interactions with the enzyme. This is more than found with any of the other inhibitors, although the P₄ BOC interaction in 1 is very weak. In addition, overall this analog has the closest interaction distances of its hydroxyl with the carboxyl oxygens at the catalytic site. There do exist, however, structural factors that may hinder the binding affinity, including the isosteric replacement (hydroxyethylene) at the P₃-P₂ linkage. Although the isostere does not replace the P₂(NH) with a hydrogen donor, 2 and 3, with a 20–80-fold enhanced potency relative to 1, do not form a hydrogen bond with Asp-77(COO) either. It therefore does not appear to be the sole reason for the low potency. As discussed above, 1 binds its phenyl group closest to the opening of the cleft region, and this may reduce the hydrophobic binding contribution and vdW contacts. Certainly the lack of both a P₂ and P₁' side chain in 1 would decrease the interaction potential. In addition, the fact that the polar P₃' group is not defined by X-ray analysis, due to being indistinguishable from solvent, indicates that it does not contribute to and actually may be counterproductive to binding. Therefore, although nine polar interactions are revealed in the crystal structure, the presence of these hydrogen bonds alone do not ensure potent binding. One must consider the lack of hydrophobic and vdW interactions in the S₂ and S₁' pockets, together with possibly reduced interactions in the S₃ and negative effects in the S₃' subsites, as having a deleterious effect on the binding energy with endothiapepsin.

Binding Activity: Renin. It is interesting to analyze the relative binding potencies of the various ligands for endothiapepsin and renin (Table I; the comparisons are approximate since they involve K₁ and IC₅₀ values). Analog 5 is the most potent inhibitor for both enzymes, although it is approximately 50 times more potent for renin. For 4 and 2, less than a 3-fold difference exists in the individual binding affinities between the two enzymes. The most significant discrepancies in activities are observed for 3 and 1. The inactivity of the phosphostatine derivative with renin has been reported to be due to the phosphinate group existing in a nonprotonated state at the optimum pH (6.0) for renin.²⁹ A repulsion therefore occurs between the phosphinate group and the diad, in which only one of the aspartic acids is protonated. Conversely, the pH optimum for endothiapepsin is in the 3.5–4.0 range, resulting in the protonation of the phosphinate oxygen. The analog in this state can bind at the active site.

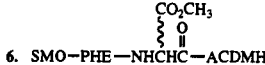
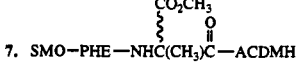
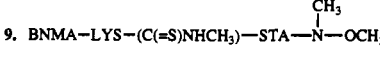
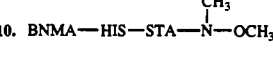
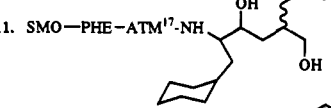
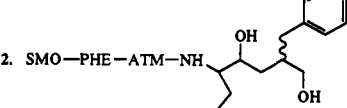
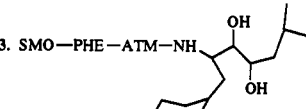
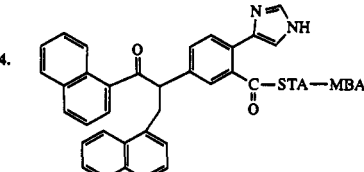
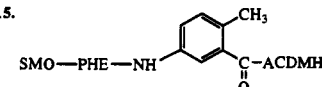
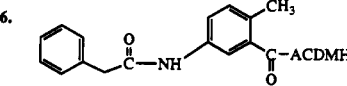
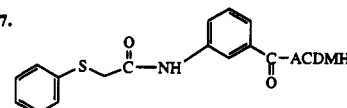
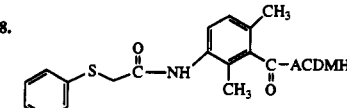
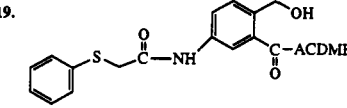
The 700-fold difference in potencies for 1 between endothiapepsin and renin remains speculative but could be attributed to a number of phenomena, including the binding of AMPMA at P₃'. As stated above, the fact that this residue is not defined in the endothiapepsin crystal

structure indicates that it is not strongly bound by the enzyme. In renin, perhaps the AMPMA can contribute to binding due to differences in the S_2' - S_3' regions of the protein relative to the fungal enzyme. A structural feature revealed in the renin crystal structure³⁰ that may affect the binding of AMPMA is the rather rigid loop segment including Pro-292-Pro-293-Pro-294, with Pro-294 and Pro-297 in a *cis* configuration. This forms a flap region that together with the loop comprised of residues 241-250, also from the C-terminal domain, and the flap segment from the N-terminal lobe cover the inhibitor in the active site. This closure from both domains resembles that found with the retroviral proteinases and differs from what is observed with the fungal enzymes, including endothiapepsin in which the Pro-292-Thr-295 renin segment is deleted. Therefore AMPMA may engage in a favorable interaction with renin and not endothiapepsin. This proposed interaction is supported by the analysis of the mouse crystal structure³⁰ (also containing a poly-Pro loop) bound with a large inhibitor extending to the P_4' subsite. The P_3' NH group of the ligand interacts with Thr-295 in the Pro loop region. Furthermore, upon a cursory evaluation of **1** in the human renin crystal structure active site, which was recently made available,³⁰ the interaction of the P_3' AMPMA group with the poly-Pro loop appears possible.

Renin Inhibitor Design. The endothiapepsin crystal structures have provided fundamental knowledge that can be applied to docking of inhibitors in the human renin enzyme model. The wealth of information gained from these crystal structures with bound inhibitors has afforded size, shape, and polar requirements and restrictions in directing the docking of inhibitors in the active site of the human renin model and in the design of novel inhibitors. Specifically, the inhibitors were manually oriented in the renin cleft guided by what was revealed by the crystal complexes regarding the transition-state mimetic complex with the aspartic acid diad, the subsite occupation and interdependencies, and the detailed polar interaction scheme. Through docking procedures, conformational analysis, and optimizations, potential inhibitors were designed and evaluated, assessing the polar interactions to guide docking and steric interactions with the enzyme cleft. The synthesis of certain analogs could be discouraged based on blatant steric incompatibility with the enzyme, while support for synthesizing compounds that were complementary to the binding site could be offered successfully on a qualitative basis. The success rate of the former predictions cannot be substantiated since normally the proposed analogs that were not considered favorable binders were not pursued. However, as will be illustrated with structure **7** (Table V), one nonsupported target compound was synthesized.

A methyl aminomalonate derivative (**6**, Table V) was found to be a potent renin inhibitor with a subnanomolar IC_{50} in vitro and moderate oral activity.³¹ Although considered a promising lead compound, concerns were raised when **6** was shown to epimerize under assay conditions at the aminomalonate residue. In an attempt to circumvent this problem, the α -methyl-substituted derivative of **6** was proposed. In the docking experiments, the P_2 group in the inhibitors was situated at a narrow neck of the binding cleft. Retaining the standard docking mode observed in the crystal structures, the addition of a methyl substituent at the P_2 α carbon resulted in an

Table V

	IC_{50} (nM) or % (M) (renin monkey plasma)
6. 	0.28
7. 	4.4% (10^{-6})
8. BNMA-LYS-(C(=S)NHCH ₃)-STA-MBA	23
9. 	10 000
10. 	62
11. 	1.7
12. 	7.7
13. 	0.4
14. 	NT ^a
15. 	4200
16. 	840
17. 	12.6% (10^{-6})
18. 	290
19. 	4.4% (10^{-6})

^a NT = not tested.

unfavorable steric contact with the enzyme (Figure 8). Therefore this substitution was not supported by molecular modeling. However, in an effort to retain the oral activity of **6** and overcome the epimerization problem, **7** was nonetheless synthesized. As can be seen in Table V, the

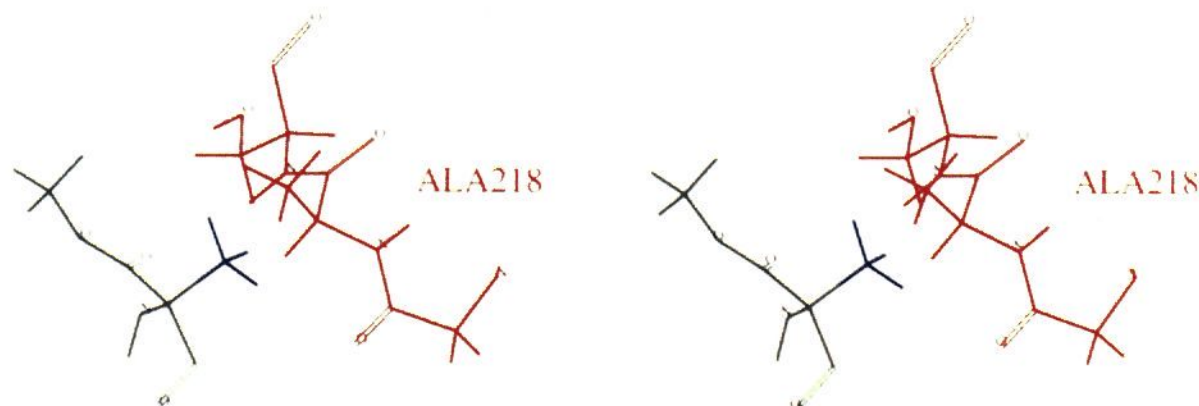


Figure 8. P₂ residue of 7 (green, α -methyl group in blue) in contact with Ala-218 (pepsin numbering) in the renin model (red).

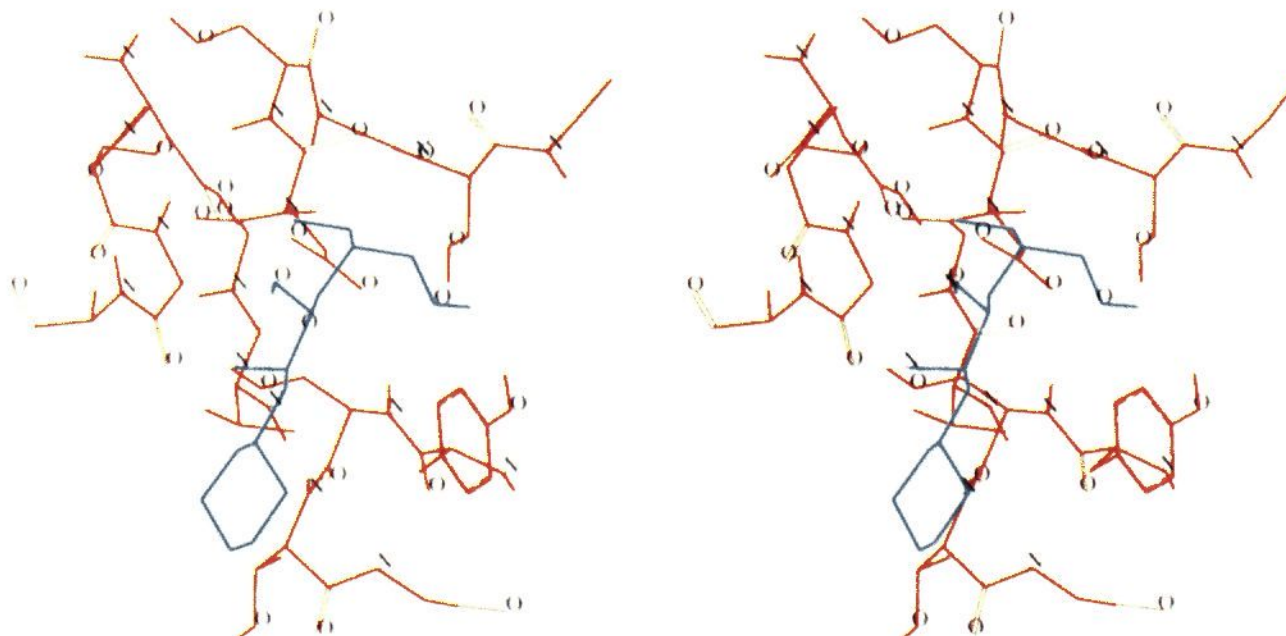


Figure 9. P₁-P₁' residue in 11 (cyan) bound in the renin enzyme model (red).

activity dropped dramatically (7 versus 6), thus strongly supporting what had been predicted from the docking experiment.

Modeling played a second role with regard to the lead compound, 6.³¹ When the epimers of 6 were isolated by fractional crystallization using the appropriate solvent, the renin inhibitory activities were found to be indistinguishable. Although these results were attributed to the epimerization occurring quickly during the testing procedure, the possibility that the individual epimers actually bind with essentially the same potency could not be definitively ruled out. Modeling studies showed that the *R* epimer, which corresponds to the L-amino acid configuration, adopted the binding pattern described for the crystal structures. However for the *S* diastereomer, binding conformations differed considerably from the crystal-based conformers. It was therefore unlikely that both the *R* and the *S* epimers would have comparable inhibitory potencies. This modeling analysis supported the premise that the near equipotent activities measured for the individual epimers resulted from rapid epimerization under assay conditions and did not reflect intrinsic relative potencies.

The interdependencies of the binding subsites described above for the crystal structures appeared evident with a series of renin inhibitors. The Lys derivative present in the P₂ site in 4 is accommodated well by both renin and endothiapepsin (Table I). Interestingly, when the P₂' MBA group in 8 was replaced with a *N,O*-dimethylamide residue (9), the renin activity decreased significantly (Table V). Molecular modeling studies³² indicated that the *N,O*-dimethylamide moiety itself was compatible with the cleft and could possibly bind in the S₁' site. However, conformational analysis of the long side chain of the Lys residue in renin showed that this residue could extend

over to the S₁' binding pocket. As described above, the S₂ and S₁' subsites are located on the same side of the inhibitor backbone. Competition by these two groups for this binding site was the rationale proposed for the diminished potency. To test this hypothesis, 10, in which the Lys residue at P₂ was replaced by a His, was synthesized. The shorter His side chain was considered less likely to interfere with the binding of the P₂' group. The IC₅₀ value for 10 was shown to be 62 nM and thus supported the proposed hypothesis for the loss of activity with 9.

The extensive information gained from the analysis of the crystal structures can be applied in the de novo design of renin inhibitors. A key interaction observed in the endothiapepsin complex with 5 is the hydrogen bond formed between Gly-76(NH) in the flap and the P₁'(OH). This directs the binding of the branched alkyl group into the P₁' pocket. This flap interaction was the basis for the design of a P₁-P₁' group, in which this hydrogen acceptor could be positioned at a different site on the ligand, as is illustrated with 11 and 12 (Table V). The modeling indicated that the diastereomers with the *S* stereochemistry at the newly formed chiral center would bind the alkyl (Figure 9) or aromatic side chains in the S₁' subsite. Simultaneously, the hydroxyl group on the terminal carbon could interact with either Ser-76(NH) in the flap region or with Gly-34(CO) in the wall of the cleft. Both of these interactions were conserved in the endothiapepsin crystal structures. Each compound was synthesized as mixture of epimers at the P₁' carbon substituted by the ethyl or benzyl side chains. As can be seen from Table V, 11 and 12 both proved to be potent inhibitors, although not quite as potent as the ACDMH compound, 13.³³ The 6-fold weaker binding of 11 relative to 13 may be linked to an entropic effect and may indicate at least equally potent

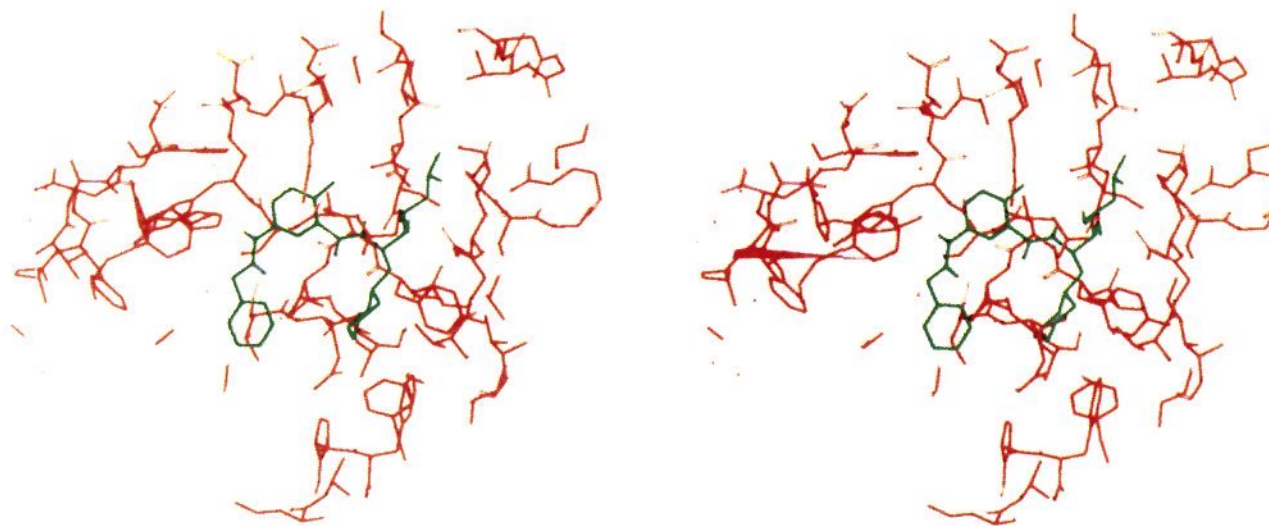


Figure 10. 16 (green) bound in the renin active-site model (red).

polar interactions. With regard to the lower affinity found for 12, modeling indicates that beyond the unfavorable entropic effect, the bulky benzyl group is not as easily accommodated by the enzyme as the smaller ethyl group in 11.

The low bioavailability of renin inhibitors has long been a concern for investigators in this field.³⁴ The peptide-like structure and size of canonical renin inhibitor molecules render these analogs susceptible to enzyme degradation, poor membrane transport, and high liver uptake. In an attempt to diverge from the standard peptide structure, 14 was designed using the renin model. This analog was later modified to a series which included 15–19. The amino terminus of 15 resulted in a tight fit when docked in the enzyme cleft. Since it was unclear whether the SMO group had polar interactions with the enzyme, the smaller benzylcarbonyl group was suggested as a replacement (16) (Figure 10). This substitution resulted in a 5-fold improvement in binding. The methyl substitution at position 2 on the phenyl ring (Table V) forces the phenyl group out of conjugation with the P₂–P₁ amide functionality. Modeling studies indicated that this effect may be necessary for binding, and therefore the drop in activity for 17 was not surprising. Modeling analysis further indicated that the phenyl ring could be substituted at position 6 and remain compatible with the cleft binding site. The substituent would push the P₃–P₂ amide out of conjugation with the phenyl system and possibly enhance a hydrogen bond between the amide carbonyl and Thr in the flap. Analog 18, which also includes an insertion of sulfur in the amino terminus, was then synthesized, and another 3-fold increase in binding potency was realized. The poor affinity of 19 could be explained by an intramolecular hydrogen bond that may form between the methylene hydroxyl and the neighboring carbonyl at position 1 of the phenyl group. This interaction would result in conformations incompatible with the standard binding mode for this series of inhibitors and thus prevent or impede binding. Analog 18 proved to be the most potent inhibitor in this series, but unfortunately this compound and 16 were not active when tested orally. The lack of oral activity may be due to the weak binding affinity and/or poor bioavailability. Actual bioavailability measurements for this series of inhibitors were not determined.

Conclusion

The analyses of the five X-ray crystal structures of the aspartic proteinase, endothiapepsin, bound with various renin inhibitors provide invaluable information regarding the enzyme active site and the multiple interactions that

take place between the protein and the ligand. The size, shape, and polarity of the protein binding region are defined by the covering of the flap segment over the cleft region. The two catalytic aspartic acid residues reside in the cleft region with their carboxyl groups aligned in a planar configuration.

The ligands bind in the active site in an extended conformation with the transition mimetic positioned tightly between the catalytic diad. Seven hydrogen bonds can be conserved between the ligand backbone and residues in the flap and wall regions of the cleft area. This pattern is characterized not only by the residues involved, but also by geometries, intermolecular distances, and hydrogen-acceptor/donor roles. Across the series of renin inhibitors analyzed, the total number of polar interactions (excluding the interactions with the diad) ranges from six to nine. On the average, the shortest hydrogen bond is formed between the Thr-219 side chain and P₃(CO), while the longest conserved hydrogen bonds involve the P₂–P₁ amide bond located toward the center of the bound ligand. This latter observation along with the revelation of the tight binding in the catalytic diad strongly suggests that the P₁–P₁' group binds first, followed by the remainder of the ligand. In the conserved hydrogen bonds with the flap residues, the hydrogen acceptors are located in the ligands, while the hydrogen donors are found in the enzyme; in all but one case, the opposite is true for the wall contacts.

The inhibitor side chains occupy enzyme subsites alternating on either side of the ligand backbone. This results in the close proximity of the S₃ and S₁ pockets, and the S₂ to both the S₄ and the S₁' subsites. Closer inspection reveals multiple binding modes within the pockets and subsite interdependencies.

By analyzing the resolved water molecules present in the complexes, insight regarding the role of solvent molecules in protein structures is gleaned. One water molecule is conserved in all the crystal structures and can interact with both the enzyme and the inhibitors. In the complexes with inhibitors lacking certain subsite side chains, water molecules reside in the unoccupied pockets, and contribute no positive entropy to binding.

The wealth of information gained through the analyses of the endothiapepsin crystal structures directs, supports, and helps develop the molecular modeling techniques and methodologies used to dock renin ligands in the human renin model and in the de novo inhibitor design. The restrictions and requirements of steric compatibility, polar complementarity, and subsite interdependencies are applied to optimization techniques, conformational analysis,

Table VI. Refinement Details for the Complexes with 4 and 5

	4	5
R factor	0.16	0.17
correlation coefficient	0.93	0.94
RMS deviation bond lengths (Å)	0.028	0.015
RMS deviation "angle-distances" (Å)	0.043	0.019
RMS deviation nonbonded contacts (Å)	0.054	0.020
RMS deviation main-chain planes (Å)	0.019	0.001
RMS deviation side-chain planes (Å)	0.012	0.001

and docking processes. The conserved hydrogen-bonding scheme pinpoints polar interaction sites that can stabilize the ligand-protein complex. The subsite description revealed by the crystal structures helps in modeling the size and shape of the newly designed inhibitors; the observed subsite interdependencies caution against focusing independently on the subsite entities. This collaboration of experimental data with molecular modeling techniques and methodologies makes possible the rational design of novel inhibitors and the screening of potentially active structures. Furthermore, a better understanding of the structure-activity relationships, as well as selectivities, that occur within the aspartic proteinase family of enzymes is realized.

Experimental Section

Crystallization. All inhibitor complexes with endothiapepsin were prepared by dissolving freeze-dried enzyme and a 10-fold molar excess of inhibitor in 0.1 M acetate buffer at pH 4.6. An enzyme concentration of 2 mg/mL was used, as this is best for crystallization of native endothiapepsin.³⁵ Due to the low solubility of some inhibitors, the solutions were stirred for at least 24 h at 4 °C to ensure that binding to the enzyme occurred. The solutions were then Millipore filtered to remove undissolved inhibitor, and finely-ground ammonium sulfate was added carefully to the point where turbidity was just visible. The solutions were Millipore filtered again and divided into 2-mL vials. Acetone was added dropwise to clear remaining turbidity. The vials were left undisturbed for a minimum of 3 months to allow growth of crystals.

X-ray Analysis. The cocrystals of endothiapepsin with 4 were of the nonisomorphous morphology⁹ with cell dimensions of $a = 43.1$ Å, $b = 75.6$ Å, $c = 42.9$ Å, and $\beta = 97.2^\circ$ belonging to space group $P2_1$. X-ray data to a resolution of 1.9 Å were collected from a single cocrystal of 4 using a Enraf-Nonius FAST area detector. The data set was merged using the Fox and Holmes algorithm³⁶ and was found to be 90% complete with a merging R value of 7.7%. The difference Fourier map revealed clear electron density for the inhibitor which was modeled using the program FRODO³⁷ and least-squares refined using RESTRAIN.³⁸ The final R factor and correlation coefficient were 0.16 and 0.93, respectively. More refinement details are given in Table VI. Cocrystals of the complex with the glycol inhibitor 5 were also of the nonisomorphous morphology ($a = 43.1$ Å, $b = 75.7$ Å, $c = 42.9$ Å, $\beta = 97.0^\circ$). Data to 1.9-Å resolution were collected using the FAST and merging (as above) resulted in a data set with a completeness of 94% and a merging R value of 5.1%. The inhibitor structure was refined to an R factor of 0.17 and correlation coefficient of 92.3% (see Table VI for more details). The X-ray analyses of 1, 2, and 3 are or will be described in detail elsewhere.^{5,10} In refinement of all the inhibitor complexes, positional parameters and isotopic temperature factors were refined for all non-hydrogen atoms. Rounds of manual rebuilding were followed by cycles of restrained refinement until convergence was achieved.

Molecular Modeling. The five crystal complexes of endothiapepsin bound with renin inhibitors were studied using the Sybyl molecular modeling software³⁹ on an Silicon Graphics 4D/35TG computer. The structures were superimposed using least-squares fitting.²⁴ Hydrogen bonds were identified by measuring the distance between the "heavy" atoms (X,Y) involved (≤ 3.6 Å) and the X-H...Y angle for which a lower limit of 90° was applied.

For each structure, a plane was defined using the six atoms of the side-chain carboxyl groups of Asp-215 and Asp-32. The RMS fit of each of the carboxylate atoms to the plane was determined. Grin/Grid calculations²³ were carried out to determine the interaction energies between a probe group and each inhibitor structure. Hydrogens were added using the Sybyl software after validating the heavy atom types. A contour was then created to map favorable interaction sites. In this study, the inhibitor crystal structures extracted from the protein were analyzed with two separate probes: a water molecule and a methyl group. The contours were created at -4 (water) and -1.5 (methyl) kcal/mol energy levels and identified polar and hydrophobic interaction sites, respectively, for each inhibitor. In the renin inhibitor design, the modeling experiments were carried out on the cleft region extracted from the renin model.^{11,12} The ligands were manually docked in the cleft guided by the crystallographic information including the bonding at the catalytic diad, the subsite occupation, and the hydrogen binding scheme. Polar and vdW contacts were evaluated through distance and, in the former case, geometry calculations. All minimizations were carried out using molecular mechanics and the Tripos force field.

Enzyme Inhibition. Measurements of the K_i values for endothiapepsin were made by use of a chromogenic octapeptide, P-P-T-I-F-NPh-R-L (where NPh = *p*-nitrophenylalanine). The hydrolysis of this substrate was measured from the average decrease in absorbance from 284 to 324 nm using a Hewlett-Packard 8452A diode array spectrophotometer.⁴⁰ Inhibitors were dissolved initially in DMSO, and all reactions were performed at 37 °C in 0.1 M sodium formate, pH 3.5, and 4% DMSO. Following preincubation of the enzyme at 37 °C for 3 min, the initial rates of six different substrate concentrations around K_m ($0.8K_m$ – $10K_m$) were measured. After preincubation with two or more inhibitor concentrations, additional curves were obtained from the initial rates from at least three different substrate concentrations. The K_i value from the family of curves was determined by Marquardt analysis and the equation $v = V_{max}[S]/[K_m(1 + [I]/K_i) + [S]]$

Inhibition of renin activity was determined by radioimmunoassay for angiotensin I, based on the method of Haber.⁴¹

In Vivo Models. Details of the protocols for high-renin normotensive²² and high-renin hypertensive⁴² monkey models have been reported.

Acknowledgment. We wish to acknowledge Dr. S. T. Rapundalo, Mr. B. L. Batley, Dr. M. J. Ryan, Mr. G. Hicks, and Mr. C. A. Painchaud for the renin in vitro and in vivo testing and Dr. C. J. Blankley for his review of the manuscript.

Supplementary Material Available: Synthetic schemes and experimental for analogs in Table V (9 pages). Ordering information is given on any current masthead page.

References

- Greenlee, W. J. Renin inhibitors. *Med. Res. Rev.* 1990, 10, 173–236.
- Wyratt, M. J.; Patchett, A. A. Recent developments in the design of angiotensin-converting enzyme inhibitors. *Med. Res. Rev.* 1985, 5, 483–531.
- Duncia, J. V.; Chiu, A. T.; Carini, D. J.; Gregory, G. B.; Johnson, A. L.; Price, W. A.; Wells, G. J.; Wong, P. C.; Calabrese, J. C.; Timmermans, P. B. M. W. M. The discovery of potent nonpeptide angiotensin II receptor antagonists: A new class of potent anti-hypertensives. *J. Med. Chem.* 1990, 33, 1312–1329.
- Hodges, J. C.; Hamby, J. M.; Blankley, C. J. Angiotensin II receptor binding inhibitors. *Drugs Future* 1992, 17, 575–593.
- Cooper, J.; Quail, W.; Frazao, C.; Foundling, S. I.; Blundell, T. L.; Humblet, C.; Lunney, E. A.; Lowther, W. T.; Dunn, B. M. X-ray crystallographic analysis of inhibition of endothiapepsin by cyclohexyl renin inhibitors. *Biochemistry* 1992, 31, 8142–8150.
- Foundling, S. I.; Cooper, J.; Watson, F. E.; Pearl, L. H.; Hemmings, A.; Wood, S. P.; Blundell, T.; Hallett, A.; Jones, D. M.; Sueiras, J.; Atrash, B.; Szelke, M. Crystallographic studies of reduced bond inhibitors complexed with an aspartic proteinase. *J. Cardiovasc. Pharmacol.* 1987, 10, S59–S68.
- Structure and Function of the Aspartic Proteinases*; Dunn, B. M., Ed.; Plenum Press: New York, 1991.

- (8) James, M. N. G.; Sielecki, A. R.; Salituro, F.; Rich, D. H.; Hoffman, T. Conformational flexibility in the active sites of aspartic proteinases revealed by a pepstatin binding to penicillopepsin. *Proc. Natl. Acad. Sci. U.S.A.* 1982, 79, 6137-6142.
- (9) Sali, A.; Veerapandian, B.; Cooper, J. B.; Moss, D. S.; Hoffman, T.; Blundell, T. L. Domain flexibility in aspartic proteinases. *PROTEINS: Structure, Function Genetics* 1992, 12, 158-170.
- (10) Dealwis, C.; Cooper, J.; Beveridge, A.; Blundell, T. L.; Humblet, C.; Hodges, J. C.; Lunney, E. A.; Lowther, W. T.; Dunn, B. M. Unpublished results.
- (11) Sibanda, B. L.; Blundell, T.; Hobart, P. M.; Fogliano, M.; Bindra, J. S.; Dominy, B. W.; Chirgwin, J. M. Computer graphics modelling of human renin. Specificity, catalytic activity and intron-exon junctions. *FEBS Lett.* 1984, 174, 102-111.
- (12) Blundell, T. L.; Sibanda, B. L.; Hemmings, A.; Foundling, S. F.; Tickle, I. J.; Pearl, L. H.; Wood, S. P. A rational approach to the design of renin inhibitors. In *Molecular Graphics and Drug Design*; Burgen, A. S. V., Roberts, G. C. K., Tute, M. S., Eds.; Elsevier Science Publishers: Amsterdam, 1986; pp 323-334.
- (13) Humblet, C.; Lunney, E. A.; Mirzadegan, T. Docking ligands in the receptor cavity What have we learned? In *Trends in Qsar and Molecular Modeling '92*; Wermuth, C. G., Ed.; Escom.: The Netherlands, 1993; pp 35-43.
- (14) The "P" subsite nomenclature relates amino acid residues or mimics in the inhibitor to corresponding residues in the natural substrate angiotensinogen. (The "S" nomenclature relates in terms of the enzyme subsites.) See: Schechter, I.; Berger, A. On the size of the active site in proteases. I. Papain. *Biochem. Biophys. Res. Commun.* 1967, 27, 157-162.
- (15) Boger, J. Renin Inhibitors. Design of angiotensinogen transition-state analogs containing statine. In *Peptides, Structure and Function. Proceedings of the Eighth American Peptide Symposium*; Hruby, V. J., Rich, D. H., Eds.; Pierce Chemical Co.: Rockford, 1983; pp 569-578.
- (16) Hutchins, C.; Greer, J. Comparative modeling of proteins in the design of novel renin inhibitors. *Crit. Rev. Biochem. Mol. Biol.* 1991, 26, 77-127.
- (17) Abbreviation follow the nomenclature of the IUPAC-IUB Joint Commission on Biochemical Nomenclature for amino acids and peptides: *Eur. J. Biochem.* 1984, 158, 9-31. Additional abbreviations are as follows: BOC = *tert*-butoxycarbonyl; MBA = 2(S)-methylbutylamine; AMPMA = *m*-bis(aminomethyl)benzene; ACD-MH = (2S,3R,4S)-2-amino-1-cyclohexyl-3,4-dihydroxy-6-methylheptane; ATM = 3-(2-amino-4-thiazolyl)alanine; SMO = 4-morpholinesulfonic acid; THF = tetrahydrofuran; DMSO = dimethyl sulfoxide; HOBT = 1-hydroxybenzotriazole; DMF = dimethylformamide; DCC = dicyclohexylcarbodiimide.
- (18) Kaltenbronn, J. S.; Hudspeth, J. P.; Lunney, E. A.; Michniewicz, B. M.; Nicolaides, E. D.; Repine, J. T.; Roark, W. H.; Stier, M. A.; Tinney, F. J.; Woo, P. K. W.; Essenburg, A. D. Renin inhibitors containing isosteric replacements of the amide bond connecting the P3 and P2 sites. *J. Med. Chem.* 1990, 33, 838-845.
- (19) Lunney, E. A.; Humblet, C. C. Comparative molecular modeling analyses of endotheiasepsin complexes as renin model templates. In *Peptides, Chemistry, Structure and Biology. Proceedings of the Eleventh American Peptide Symposium*; Rivier, J. E., Marshall, G. R., Eds.; ESCOM: Leiden, 1990; pp 387-389.
- (20) Doherty, A. M.; Kaltenbronn, J. S.; Hudspeth, J. P.; Repine, J. T.; Roark, W. H.; Sircar, I.; Tinney, F. J.; Connolly, C. J.; Hodges, J. C.; Taylor, M. D.; Batley, B. L.; Ryan, M. J.; Essenburg, A. D.; Rapundalo, S. T.; Weishaar, R. E.; Humblet, C.; Lunney, E. A. New inhibitors of human renin that contain novel replacements at the P2 site. *J. Med. Chem.* 1991, 34, 1258-1271.
- (21) Doherty, A. M.; Hamilton, H. W.; Hodges, J. C.; Repine, J. T. U.S. Patent Number 5,063,207, 1991.
- (22) Repine, J. T.; Kaltenbronn, J. S.; Doherty, A. M.; Hamby, J. M.; Himmelsbach, R. J.; Kornberg, B. E.; Taylor, M. D.; Lunney, E. A.; Humblet, C.; Rapundalo, S. T.; Batley, B. L.; Ryan, M. J.; Painchaud, C. A. Renin inhibitors containing α -heteroatom amino acids as P2 residues. *J. Med. Chem.* 1992, 35, 1032-1042.
- (23) Grin/Grid Software, Molecular Discovery Ltd., West Way House, Elms Parade, Oxford, OX2 9LL, England.
- (24) Sali, A.; Blundell, T. L. The definition of topological equivalence in homologous and analogous structures: A procedure involving comparison of local properties and structural relationships through simulated annealing and dynamic programming. *J. Mol. Biol.* 1990, 212, 403-428.
- (25) Foundling, S. I.; Cooper, J.; Watson, F. E.; Cleasby, A.; Pearl, L. H.; Sibanda, B. L.; Hemmings, A.; Wood, S. P.; Blundell, T. L.; Valler, M. J.; Norey, C. G.; Kay, J.; Boger, J.; Dunn, B. M.; Leckie, B. J.; Jones, D. M.; Atrash, B.; Hallett, A.; Szelke, M. High resolution X-ray analyses of renin inhibitor-aspartic proteinase complexes. *Nature* 1987, 327, 349-352.
- (26) Luly, J. R.; BaMaung, N.; Soderquist, J.; Fung, A. K. L.; Stein, H.; Kleierner, H. D.; Marcotte, P. A.; Egan, D. A.; Bopp, B.; Merits, I.; Bolis, G.; Greer, J.; Perun, T. J.; Plattner, J. J. Renin inhibitors. Dipeptide analogs of angiotensinogen utilizing a dihydroxyethylene transition-state mimic at the scissile bond to impart greater inhibitory potency. *J. Med. Chem.* 1988, 31, 2264-2276.
- (27) Rosenberg, S. H.; Dellaria, J. F.; Kempf, D. J.; Hutchins, C. W.; Woods, K. W.; Maki, R. G.; De, L. E.; Spina, K. P.; Stein, H. H.; Cohen, J.; Baker, W. R.; Plattner, J. J.; Kleierner, H. D.; Perun, T. J. Potent, low molecular weight renin inhibitors containing a C-terminal heterocycle: hydrogen bonding at the active site. *J. Med. Chem.* 1990, 33, 1582-1590.
- (28) Boger, J.; Payne, L. S.; Perlow, D. S.; Lohr, N. S.; Poe, M.; Blaine, E. H.; Ulm, E. H.; Schorn, T. W.; LaMont, B. I.; Lin, T.-Y.; Kawai, M.; Rich, D. H.; Veber, D. F. Renin inhibitors. Synthesis of subnanomolar, competitive, transition-state analogue inhibitors containing a novel analogue of statine. *J. Med. Chem.* 1985, 28, 1779-1790.
- (29) Allen, M. C.; Fuhrer, W.; Tuck, B.; Wade, R.; Wood, J. M. Renin inhibitors. Synthesis of transition-state analogue inhibitors containing phosphorus acid derivatives at the scissile bond. *J. Med. Chem.* 1989, 32, 1652-1661.
- (30) Dhanaraj, V.; Dealwis, C. G.; Frazao, C.; Badasso, M.; Sibanda, B. L.; Tickle, I. J.; Cooper, J. B.; Driessen, H. P. C.; Newman, M.; Aguilar, C.; Wood, S. P.; Blundell, T. L.; Hobart, P. M.; Geoghegan, K. F.; Ammirati, M. J.; Danley, D. E.; O'Connor, B. A.; Hoover, D. J. X-ray analyses of peptide-inhibitor complexes define the structural basis of specificity for human and mouse renins. *Nature (London)* 1992, 357, 466-472.
- (31) Repine, J. T.; Himmelsbach, R. J.; Hodges, J. C.; Kaltenbronn, J. S.; Sircar, I.; Skeean, R. W.; Brennan, S. T.; Hurley, T. R.; Lunney, E. A.; Humblet, C. C.; Weishaar, R. E.; Rapundalo, S. T.; Ryan, M. J.; Taylor, D. G.; Olson, S. C.; Michniewicz, B. M.; Kornberg, B. E.; Belmont, D. T.; Taylor, M. D. Renin inhibitors containing esters at the P₂-position. Oral activity in a derivative of methyl aminomalonate. *J. Med. Chem.* 1991, 34, 1935-1943.
- (32) Lunney, E. A.; Humblet, C. C.; Repine, J. T.; Blundell, T. L.; Cooper, J. B.; Sibanda, B. L. Molecular modeling of renin inhibitor P₂ substituents. *Adv. Exp. Med. Biol.* 1991, 391-394.
- (33) Patt, W. C.; Hamilton, H. W.; Taylor, M. D.; Ryan, M. J.; Taylor, D. G.; Connolly, C. J. C.; Doherty, A. M.; Klutchko, S. R.; Sircar, I.; Steinbaugh, B. A.; Batley, B. L.; Painchaud, C. A.; Rapundalo, S. T.; Michniewicz, B. M.; Olson, S. C. Structure-activity relationships of a series of 2-amino-4-thiazole-containing renin inhibitors. *J. Med. Chem.* 1992, 35, 2562-2572.
- (34) Weidmann, B. Renin inhibitors. From transition state analogs and peptide mimetics to blood pressure lowering drugs. *Chimia* 1991, 45, 367-376.
- (35) Moews, P. C.; Bunn, C. W. An X-ray crystallographic study of the renin-like enzyme of *Endothia parasitica*. *J. Mol. Biol.* 1970, 54, 395-397.
- (36) Fox, G. C.; Holmes, K. C. An alternate method of solving the layer scaling equations of Hamilton, Rollet & Sparks. *Acta Crystallogr.* 1966, A20, 886-891.
- (37) Jones, A. T. A graphics model building and refinement system for macromolecules. *J. Appl. Crystallogr.* 1978, 11, 268-272.
- (38) Haneef, I.; Moss, D. S.; Stanford, M. J.; Borkakoti, N. Restrained structure factor least squares refinement of protein structures using a vector processing supercomputer. *Acta Crystallogr.* 1985, A41, 426-433.
- (39) Sybyl Molecular Modeling Software, Versions 3 and 5, Tripos Associates Inc., A subsidiary of Evans and Sutherland, 1699 S. Hanley Rd., Suite 303, St. Louis, MO 63144.
- (40) Dunn, B. M.; Jimenez, M.; Parten, B. F.; Valler, M. J.; Rolph, C. E.; Kay, J. A systematic series of synthetic chromophoric substrates for aspartic proteinases. *Biochem. J.* 1986, 237, 899-906.
- (41) Haber, E.; Koerner, T.; Page, L. B.; Kliman, B.; Purnode, A. Application of a radioimmunoassay for angiotensin I to the physiological measurements of plasma renin activity in normal human subjects. *J. Clin. Endocrinol.* 1969, 29, 1349-1355.
- (42) Panek, R. L.; Ryan, M. J.; Weishaar, R. E.; Taylor, D. G. Development of a high renin model of hypertension in the cynomolgus monkey. *Clin. Exper. Hyper.-Theory Practice* 1991, A13, 1395-1414.